IL NUOVO CIMENTO **48 C** (2025) 24
DOI 10.1393/ncc/i2025-25024-3

Colloquia: WPCF-Resonance 2023

Searching for the X17 with the PADME experiment

F. Ferrarotto(*) on behalf of the PADME Collaboration
INFN, Sezione di Roma 1 - Roma, Italy

received 23 July 2024

Summary. — Certain classes of dark matter theories predict the existence of a new, hidden "Dark Sector" of particles which interact with Standard Model particles only through the exchange of a new, massive mediator. This is the scenario that the Positron Annihilation into Dark Matter Experiment (PADME) was originally designed to test using the positron beam at the Beam Test Facility (BTF) at the INFN Laboratori Nazionali di Frascati (LNF). The confirmation of the X17 anomaly in 2021, observed in internal pair creation nuclear decays at the ATOMKI institute in Debrecen, Hungary, kindled significant interest within the particle physics community. Assuming that the anomaly comes from the decay of a new particle to an e^+e^- pair, time-reversal symmetry implies that the new particle must be producible in e^+e^- annihilation. Since the beam used at PADME is the only one worldwide with the correct energy to create this new particle on resonance, the PADME collaboration pivoted to study the X17 anomaly in the reaction $e^+e^- \to X17 \to e^+e^-$, aiming to confirm/disprove the particle hypothesis. In 2022, PADME Run III was dedicated specifically to this search. Approximately 10^{10} positrons on target were collected for each of the 47 beam energy values in the range $262 \div 298$ MeV. This paper gives an overview of the scientific program of the experiment and of the data analyses ongoing.

1. – The dark sector paradigm

In Dark Matter studies, the absence of experimental evidences not coming from astrophysical observations has triggered new approaches. Nowadays, many particle physics experiments at accelerators are trying to contribute by looking for signals of hidden particles postulated by different theoretical extensions of the Standard Model (SM).

If a Dark Sector (DS) exists, its mediator candidates can have a small mass (0 MeV -100 MeV) and can be produced at low energy particle accelerators.

In the case of DS models with a hidden $U'(1)$ extension, the mediator will be a massive boson (the so-called Dark Photon A') which can decay to ordinary matter ("visible" decay) or to dark matter ("invisible" decay).

(*) E-mail: fabio.ferrarotto@roma1.infn.it

It can be produced by electron beams only by "A'-strahlung" (similar to Bremsstrahlung, but with the SM photon replaced by the A') or it can be produced by positron beams by "A'-strahlung" , associate production $ee \rightarrow A'\gamma$ or resonant production $ee \rightarrow A'$.

2. – The PADME Experiment and setup (Run I and Run II)

The Positron Annihilation into Dark Matter Experiment (PADME) at the Beam Test Facility (BTF) of the Laboratori Nazionali di Frascati of INFN, is searching for dark sector candidates by studying the annihilations of the BTF positrons beam with the electrons of a fixed target [1]. The PADME physics program includes, together with the dark photon search, Axion-Like-Particles (ALPs), proto-phobic X bosons and Dark Higgs investigations.

Furthermore, thanks to its peculiar center of mass energy range, PADME has an unmatchable potential in ruling out or confirming the existence of the anomaly observed in the decays of highly excited nuclear states in the large opening angle of Internal Pair Creation (IPC) e^+e^- produced at ATOMKI [2-4].

This anomaly (named the X17 boson) might be produced via the resonant annihilation process: $e^+e^- \rightarrow X17$ [5] and then identified through its decay via e^+e^-. In this paper we report an overview of the PADME detector and of the beam-line optimization performed to allow a dedicated data taking at beam energies around 282 MeV, meant to produce the X17 at resonance.

The PADME detector was designed to investigate the associated production of a dark photon A' together with an ordinary photon. The positron beam from the BTF (maximum energy of 550 MeV, intensity 30 K particles/bunch, frequency = 50 Hz) impinges on a 100 μm thick active diamond target that allows to measure the beam intensity and the impact position. In the positron-target interaction, the production of a dark photon can actually occur via different mechanisms: resonant production, associated production or "A'-strahlung".

PADME is mainly studying associated production by selecting events where a single SM photon is detected by the Electromagnetic Calorimeter (ECAL, consisting of an array of 616 BGO crystals read by PMTs) and nothing else is present in all the other detectors in a time interval of $\pm$ 2 ns (see fig. 1). The mass $M_{A'}$ would possibly emerge as a peak in the missing mass distribution of this process.

The main source of background is represented by SM Bremsstrahlung (producing photons emitted at low angles to the beam). For this reason the ECAL was built with a central hole, which is where the Small Angle Calorimeter (SAC, made of 25 PbF_2 crystals read by fast PMTs) is situated. The SAC information, having a faster response time than ECAL, combined with the one of the Charged Particle Vetoes, enables to cut out the high flux of Bremsstrahlung photons. The Vetoes consists of three stations of plastic scintillator sticks read by SiPMs: two are located along the walls of the vacuum vessel inside the 0.5 T dipole, while the third is located near the beam exit window.

The experimental setup is completed by a silicon pixel detector (TimePix3 [6]) used as beam monitor, located on the outgoing path of not-interacting positrons. More details about the PADME detector can be found in [7].

In the period between September 2019 and December 2020 PADME has performed 2 runs in 3 different configurations.

Using part of the Run II data PADME published [8] the first direct measurement below 500 MeV of the $e^+e^- \rightarrow \gamma\gamma(\gamma)$ cross section with a ~ 5 % precision (both Colgate

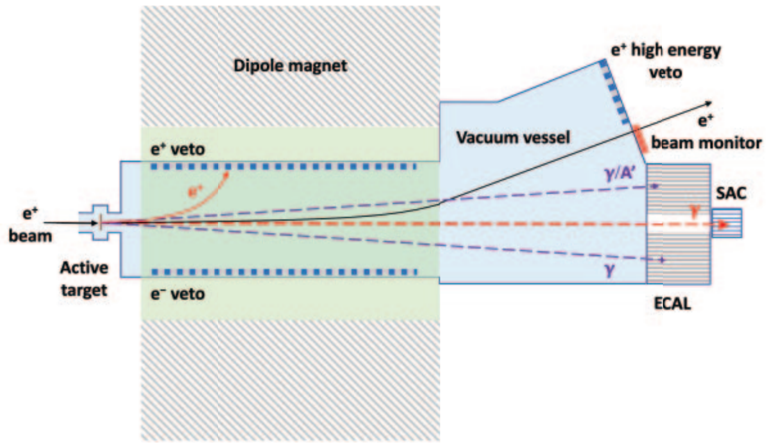

Fig. 1. – PADME detector layout for Run I and Run II with main detectors shown. A "golden" $A'\gamma$ associated production event with an undetected A' is shown in violet and a Bremmstrahlung event is shown in red.

et al. [9] and Malamud et al. [10] measured only e^+ disappearance rate):

$$\sigma(e^+e^- \to \gamma\gamma(\gamma)) = (1.977 \pm 0.018\ stat \pm 0.012\ syst)\ \text{mb}$$

in very good agreement with the QED@NLO calculation by Balossini et al. [11]:

$$\sigma(e^+e^- \to \gamma\gamma(\gamma)) = (1.9478 \pm 0.0005\ stat \pm 0.0020\ syst)\ \text{mb}$$

This measurement represents a fundamental step towards the invisible dark photon analysis, still ongoing.

3. – The X17 particle

While studying the de-excitation via IPC of ^8Be nucleus an Hungarian group of the ATOMKI Institute of Debrecen announced in 2016 the presence of a 6.8 σ anomaly [2] in the opening angle of the measured e^+e^- pairs, later confirmed by other experiments on ^4He (2021) [3] and ^{12}C (2022) [4] nuclei.

The attempt to explain these observations triggered a lot of theoretical speculation. Among others, Feng et al. [12] put forward the possibility that the effect could be an indication of a protophobic new particle of mass approximately 17 MeV/c^2.

All the observed experimental excesses are in fact compatible with a new particle (named the "X17") of mass roughly 17 MeV/c^2 decaying to e^+e^- that can indicate the existence of a new force of nature.

From the ATOMKI observations, the main properties of the new X17 particle are:
- It is proto-phobic (Feng et al. [12])
- M(X17) $\sim$ 17 MeV/c^2 (compatible in all 3 experiments)
- $Br(e^+e^- \to X17) \sim 5 \times 10^{-6}\ Br(e^+e^- \to \gamma\gamma)$
- $\Gamma_V \sim 0.5\ (g_V/0.001)^2\ < 10^{-2}$ eV (for the vector case)

The X17 hypothesis is kinematically consistent for all the 3 experiments, as reported by [13], by using all 11 angular measurements and fitting with a simple angular relation

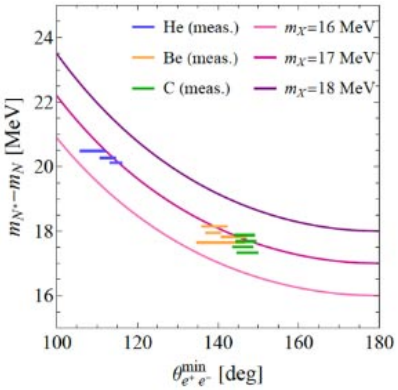

N_*	J^P_*	Scalar X17	Pseudoscalar X17	Vector X17	Axial Vector X17
^{8}Be(18.15)	1^+	✗	✓	✓	✓
^{12}C(17.23)	1^-	✓	✗	✓	✓
^{4}He(21.01)	0^-	✗	✓	✗	✓
^{4}He(20.21)	0^+	✓	✗	✓	✗

^{12}C Last results

Fig. 2. – Left: Kinematical fit of X17 angular distributions [13]. Right: J^{PC} assignment table for X17 resumed from [14].

$\theta_{ee}^{min} \sim 2arcsin(m_{X17}/m_{N\star} - m_N)$ a value for the mass $M_X = 16.85 \pm 0.04$ MeV/c^2 is obtained, as shown in the left panel of fig. 2.

In the right panel of fig. 2 we have resumed the results by Feng et al. [14] showing the table of preferred J^{PC} assignments for all 3 experiments. Considering all experimental results the assignment to a vector or an axial-vector particle seems to be preferred, excluding a scalar or pseudoscalar one.

Very recently a new result has been reported [15] with the observation of the X17 anomaly in the decay of the ^8Be Giant Dipole Resonance.

4. – Search for X17 using resonant production on thin target

PADME performed in 2022 a dedicated Run III to study the X17 particle: the idea was to use the resonant production and search for visible $X17$ decay into e^+e^- [5]. PADME@LNF is actually the only facility having a positron beam of the proper energy capable to do this measurement.

The resonant production scales only with Z and it is much larger than the associated and radiative production (BW enhancement). To exploit this feature the center of mass energy should be as close as possible to the expected mass: $E_{res} = M^2_{X17}/m_e$, thus an energy scanning procedure is needed.

The measurement strategy is: vary the beam energy, evaluate the background, calibrate the luminosity and look for a resonance peak over the background.

The main expected backgrounds are from Bhabha scattering and $\gamma\gamma$ production and can be fitted directly from data.

For NPoT $= 10^{11}$ and a beam of energy $E_{beam} = 282$ MeV ($\sqrt{s} \sim 17$ MeV), using simple cuts on both final state particles, Darmé et al [5] obtained the table in fig. 3 for the expected number of events and efficiencies using for signal and background reactions the following parameters:

- Azimuthal angle: 25.5 mrad $< \theta_{1,2} <$ 77 mrad
- final state e^+ e^- energy E_e $>$ 100 MeV
- assumed detector efficiency $\sim$ 100 %
- X17 coupling $g_{ve} = 2 \times 10^{-4}$ and beam energy spread $\delta E = 1.4$ MeV

A resonant signal should emerge on top of the Bhabha BG in one or more points of the energy scan.

BG process	No. of Ev.	No. of Ev. in Acc.	Acc.
$e^+e^- \to e^+e^-$ (t- ch.)	5.4×10^7	6.9×10^4	0.13%
$e^+e^- \to e^+e^-$ (s- ch.)	3.2×10^4	6.4×10^3	20%
$e^+e^- \to \gamma\gamma$	2.9×10^5	1.3×10^4	4.5%
$e^+e^- \to X_{17} \to e^+e^-$	1250	250	20%

Fig. 3. – Production estimates for X17 and backgrounds in [5].

The background from SM Bhabha scattering must be kept under control down to few 10^{-4}. The challenges are to achieve an extremely precise luminosity measurement and systematic errors control ($< 1\%$) with order of 10^{10} PoT per each scan point.

Under these assumptions, PADME aims to set limits both on:

- vector model, covering almost the entire free parameter space, where PADME has the maximum sensitivity;

- pseudoscalar model, in the case of an ALPs decaying into leptons only.

5. – The Run III experimental setup

Improvements to the PADME set-up were necessary for the X17 resonant search, since the use of PADME vetos to reconstruct e^+e^- pairs not originated in the target is impossible.

The idea was then to identify e^+e^- using the ECAL calorimeter, as in $\gamma\gamma$ events, switching off the magnetic field to get both final state particles in ECAL.

To distinguish ee from $\gamma\gamma$ final states a charged particle detector (ETag), consisting of a wall of 5 mm plastic scintillators read out on both sides by SiPMs, was placed in front of the ECAL (see fig. 4).

Furthermore, the SAC calorimeter was replaced by a beam monitor system consisting of the TimePix3 detector (providing offline a precise evaluation of beam energy and intensity) followed by a LeadGlass crystal with PMT readout (used to monitor online the beam energy and intensity).

Changing the current of the first dipole in the BTF beam line the beam energy is selected, while the current tuning in the second one is used to correct the final beam trajectory and center it on the PADME axis (see fig. 5).

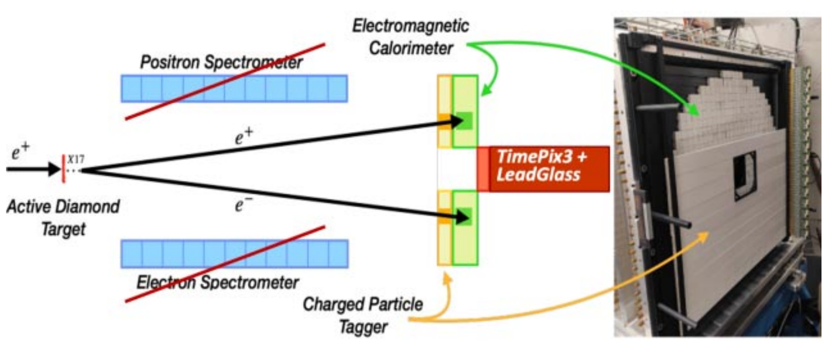

Fig. 4. – Padme detector layout for Run III.

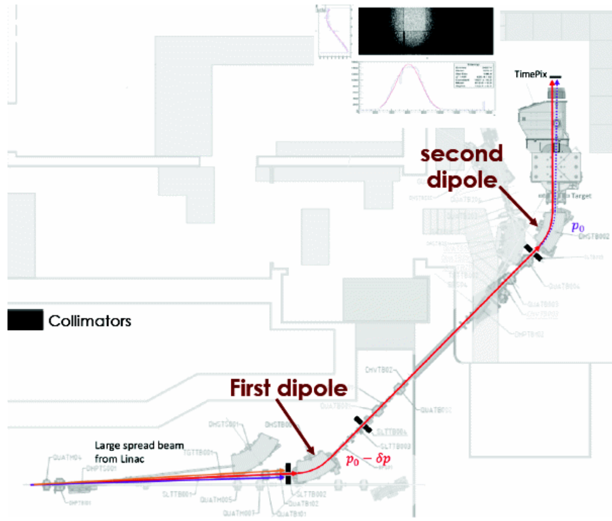

Fig. 5. – BTF Beam line setup.

In order to reduce the pile-up and have a better energy resolution the beam intensity of Run III was reduced with respect to Run II by a factor 10.

The main beam parameters for all Run III were:

- Beam bunch length $\sim$ 200-250 ns ,
- N_{PoT}/bunch $\sim$ 2500,
- Beam frequency $f \sim 50$ Hz.

The total amount of data collected during Run III is $\sim\ 6 \times 10^{11}\ N_{PoT}$, *i.e.*, $\sim 10^{10}$ PoTs/point in 47 invariant mass points in the beam energy range 262 MeV $< E_{beam} <$ 298 MeV ($\pm 2\sigma$ around the expected mass by Atomki) with $\delta E_{beam} \sim 0.75$ MeV (see fig. 6).

Six data points out-of resonance were also collected: 5 points at different energies below resonance + 1 above resonance (5 separate runs) to estimate the SM background and systematics, and 4 points at different energies without target for beam background estimates.

6. – Off-resonance data and beam background estimates

The data analysis started with the evaluation of the number of events with 2 clusters/N_{PoT} (($N(2cl)/N_{PoT}$), determined using a selection of 2 clusters ($e^+e^-\ +\ \gamma\gamma$) observed in ECal (no need to rely on Etag efficiency). This variable has the highest statistical significance and the systematics depend only on the luminosity.

A peak found over background in this variable in the energy scan will be a proof for the existence of the X17.

A first selection has been made for data above and below the resonance region (see fig. 7), identifying pairs of clusters in time in ECal ($\Delta t < 5$ ns), $E_{cl} > 75$ MeV.

For both data sets the kinematic relation between the cluster energy and the cluster Theta angle shows a very well defined region (inside the red lines) compatible with a 2-body final state, which separates well from the background region.

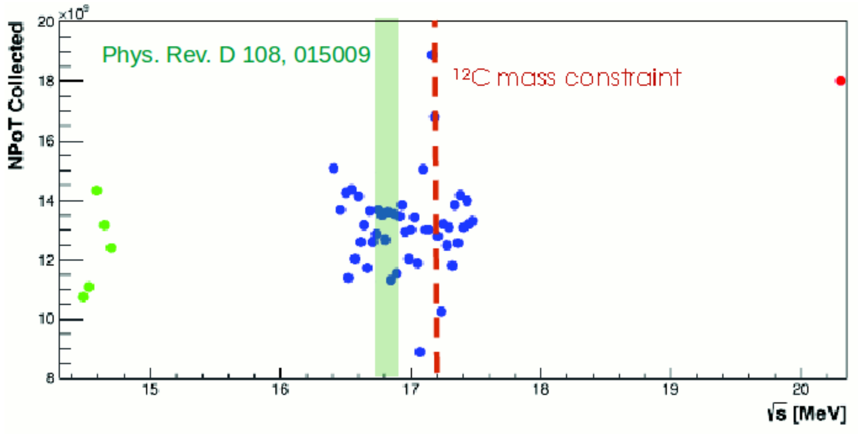

Fig. 6. – PADME Run III (2022) data set collection *vs.* Center-of-mass Energy. - Blue, green and red points: energies scanned by PADME in the resonance region (blue), below (green) and above (red). - Green shaded area: mass interval for X17 from the fit in [13]. - Red dotted line: mass limits for X17 from [4].

The beam background contribution (outside the red lines in fig. 7) seem under control in both energy regions.

Figure 8 shows also a preliminary stability study of $N(2cl)/N_{PoT}$ for data over and below the resonance region.

In fig. 8 left the reconstructed values of $N(2cl)/N_{PoT}$ for the 5 runs at $E_{beam} = 402$ MeV (no acceptance corrections applied yet) shows errors are all compatible with pure statistics contribution with no significant systematics, and the constant fit has a good χ^2.

In fig. 8 right for the 5 runs with $205 < E_{beam} < 212$ MeV $N(2cl)/N_{PoT}$ exhibits a linear trend (due to different acceptances for the various energies) well reproduced by MC. The linear fit (no acceptance corrections applied yet) has a good χ^2 with RMS $<$ 1% over all points, computed on residuals wrt to the fit.

In fig. 9 $N(2cl)/N_{PoT}$ is shown for the 4 data sets taken at different beam energies without target. Running the same selection code on no-target data an estimate of the contamination from beam background in the signal selection is performed.

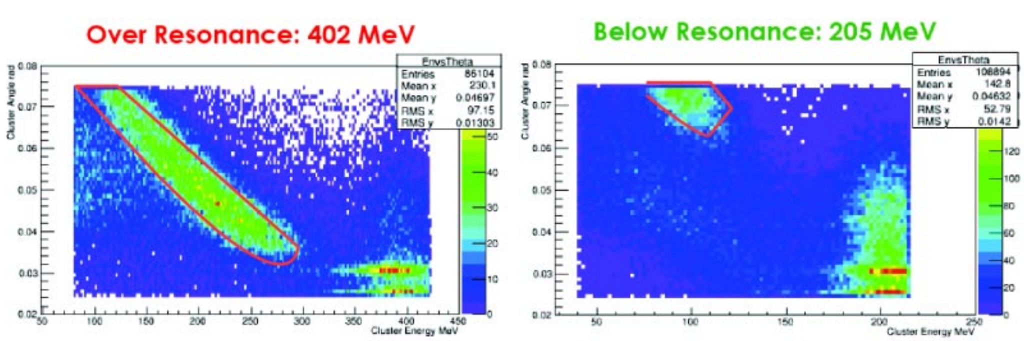

Fig. 7. – PADME Run III Cluster Energy *vs.* Theta Angle for data above (left, E_{beam}=402 MeV) and below (right, E_{beam}=205 MeV) resonance.

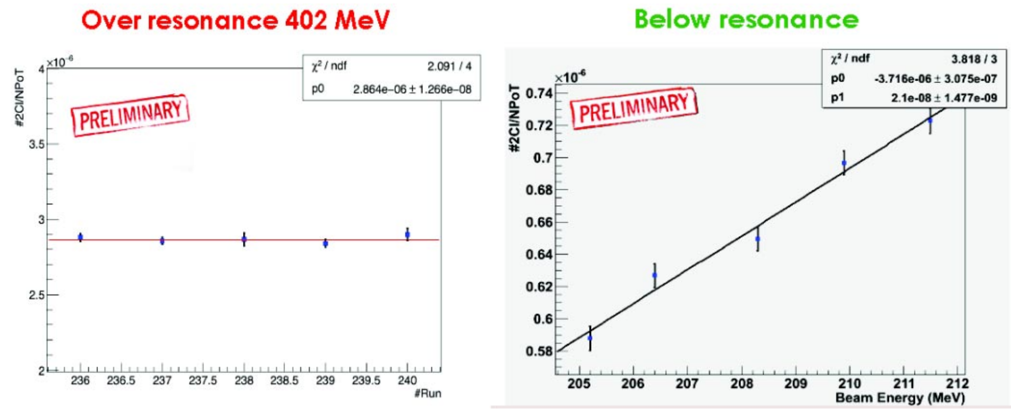

Fig. 8. – Left: $N(2cl)/N_{PoT}$ *vs.* Number of run; $E_{beam} = 402$ MeV. Right: $N(2cl)/N_{PoT}$ *vs.* Beam energy: $205 < E_{beam} < 212$ MeV.

The observed ratio of $N(2cl)/N_{PoT}$ between no-target data and data off-resonance is a few permille, showing that the beam background is small and stable.

7. – Conclusions

PADME Run III scan for the search of the X17 particle was successfully made in 2022.

High quality data (47 points) have been collected for 262 MeV $< E_{beam} <$ 298 MeV (16.35 MeV $< \sqrt{s} <$ 17.5 MeV), plus 5 more points at $205 < E_{beam} < 212$ MeV (below resonance) , 1 more point at $E_{beam} = 402$ MeV (above resonance) and 4 points without target at $268 < E_{beam} < 295$ MeV.

Beam Background and Bhabha contributions are both under control and data quality is good.

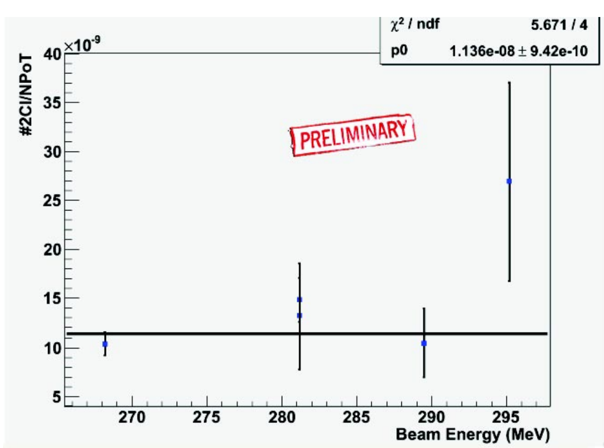

Fig. 9. – $N(2cl)/N_{PoT}$ *vs.* E_{beam}; data taken without the target in the beam line at 4 different energies.

* * *

The PADME Collaboration wishes to thank the LNF LINAC team and all the accelerator division for the excellent efficiency and quality of the machine operation during PADME Run III.

REFERENCES

[1] Raggi M. and Kozhuharov V., *Adv. High Energy Phys.*, **2014** (2014) 959802.
[2] Krasznahorkay A. J. *et al.*, *Phys. Rev. Lett.*, **116** (2016) 042501.
[3] Krasznahorkay A. J. *et al.*, *Phys. Rev. C*, **104** (2021) 044003.
[4] Krasznahorkay A. J. *et al.*, *Phys. Rev. C*, **106** (2022) L061601.
[5] Darmé L., Mancini M., Nardi E. and Raggi M., *Phys. Rev. D*, **106** (2022) 115036.
[6] Frojdh E., Campbell M., Gaspari M. D., Kulis S., Llopart X., Poikela T. and Tlustos L., *JINST*, **10** (2015) C01039.
[7] Albicocco P. *et al.*, *JINST*, **17** (2022) P08032.
[8] PADME Collaboration, *Phys. Rev. D*, **107** (2023) 012008.
[9] Colgate S. A. and Gilbert F. C., *Phys. Rev.*, **89** (1953) 790.
[10] Malamud E. and Weill R., *Nuovo Cimento*, **27** (1953) 418.
[11] Balossini G. *et al.*, *Phys. Lett. B*, **663** (2008) 209.
[12] Feng J. L., Fornal B., Galon I., Gardner S., Smolinsky J., Tait T. M. P. and Tanedo P., *Phys. Rev. Lett.*, **117** (2016) 071803.
[13] Denton P. B. and Gehrlein J., *Phys. Rev. D*, **108** (2023) 015009.
[14] Feng J. L. ,Tait T. M. P. and Verhaaren C. B., *Phys. Rev. D*, **102** (2020) 036016.
[15] Krasznahorkay A. J. *et al.*, arXiv:2308.06473 [nucl-ex] (2023).